Functionalisation of Hollow Gold Nanospheres for use as Stable, Red-shifted SERS Nanotags

Cite this: DOI: 10.1039/x0xx00000x

S. Moreton,[a] Karen Faulds,[a] Neil C. Shand,[b] Matthew A. Bedics,[c] Michael R. Detty[c] and Duncan Graham*[a]

Received ooth January 2012,
Accepted ooth January 2012

DOI: 10.1039/x0xx00000x

www.rsc.org/

Hollow Gold Nanospheres (HGNs) exhibit a unique combination of properties which provide great scope for their use in many biomedical applications. However, they are highly unstable to changes in their surrounding environment and have a tendency to aggregate, particularly when exposed to high salt concentrations or changes in pH which is not ideal for applications such as cell imaging and drug delivery where stable solutions are required for efficient cellular uptake. Therefore there is a significant need to find a suitable stabilising agent for HGNs, however potential stabilising agents for these nanostructures have not previously been compared. Within this work we present an improved method for stabilising HGNs which simultaneously shifts the SPR from around 700 nm to 800 nm or greater. Herein, we compare three different materials which are commonly used as stabilising agents; polymers, sugars and silica in order to determine the optimum stabilising agent for HGNs. Analysis was performed using extinction spectroscopy and dynamic light scattering, supported with SEM imaging. Results showed PEG to be the most suitable stabilising agent for HGNs displaying both an increased stability to changes in salt concentration and pH as well as increased long term stability in solution. Furthermore, we demonstrate that in addition to increased stability, SERS detection can be achieved at both 1064 nm and 785 nm excitation. This combination of improved stability with a SPR in the NIR region along with SERS detection demonstrates the great potential for these nanostructures to be used in applications such as biological SERS imaging and drug delivery.

Introduction

Hollow gold nanospheres (HGNs) are unique nanostructures which consist of a thin gold shell with a hollow interior.[1] As with all nanomaterials consisting of the coinage metals, they display a strong surface plasmon band in their extinction spectra. This surface plasmon resonance (SPR) arises due to the collective oscillation of valence electrons which occurs in the presence of an applied electric field.[2] As the SPR is sensitive to changes in size, shape, and particle homogeneity, changes in nanoparticle functionality can be closely monitored using extinction spectroscopy. [3, 4] HGNs possess a highly tunable SPR, careful control of particle size and wall thickness during the synthesis can result in SPRs from 550 nm to 1320 nm. [1, 5, 6] This tunability to NIR wavelengths along with their small size and spherical shape makes HGNs of great interest for use in many potential biomedical applications including photothermal ablation therapy (PTA) and drug delivery. [3, 7] Their NIR SPR also gives them great scope for use as substrates in surface-enhanced Raman scattering (SERS) which is a highly sensitive spectroscopic technique used to detect molecules in close proximity to a metal surface.[8] The development of stable SERS substrates in the NIR region are of great interest in biomedical applications as light at wavelengths between 800 and 1200 nm can penetrate human tissue and blood, thus providing a transparent sensing window.[9, 10]

However, their use in these aforementioned applications may be hindered by the fact that they have a tendency to aggregate when exposed to changes in the surrounding environment such as high salt concentration or changes in pH. Stability to changes in pH is of particular importance in biomedical applications due to the large variations in pH throughout the body, ranging from pH 2 in the stomach, pH 7.4 to 5.4 in cancerous tissues and pH 5-8 in the intestine.[11] Although aggregation can prove advantageous for applications such as SERS, uncontrolled aggregation will cause limited reproducibility in SERS signals.[8] Additionally, stable colloids are particularly desirable in applications such as drug delivery where monodisperse nanoparticles below 100 nm in size are required for efficient cellular uptake.[12]

There are a wide variety of materials frequently used to functionalise nanoparticles which provide increased stability and improved biocompatibility. For example, polymers such as polyethylene glycol (PEG) have previously been shown to improve long term stability of gold nanoparticles and increase their stability to high salt concentrations similar to those found in vivo.[13, 14] Sugars such as thioglucose can enhance cellular uptake and provide the nanoparticles with a hydrophilic monolayer which aids stabilisation against aggregation.[3, 15, 16] Silica is another excellent coating material for nanoparticles due to its highly understood surface chemistry which can be further manipulated to produce nanostructures with a high

biocompatibility, as well as its high stability to most organic solvents and optical transparency.[17-19] Additionally, silica coated nanoparticles can maintain high spectroscopic activity after long term storage.[20, 21]

HGN synthesis is based upon a galvanic reaction whereby cobalt (Co) nanoparticles are used as sacrificial templates for growth of the gold shell.[1, 5] Citrate is generally used as a final capping agent to stabilise HGNs however within this work it was found that they showed a degree of instability both over time and in response to external stimuli. Zhang *et al*. reported that poly(vinylpyrrolidone) (PVP) can effectively stabilise HGNs.[22] PVP was added to stabilise Co nanoparticles prior to the addition of gold in the synthesis in order to slow down the growth of the shell, resulting in both an increase in nanoparticle stability and a shift in SPR to longer wavelengths. However, it was reported that this method solely worked for PVP and other polymers tested were unsuccessful.[22] Further to this work, we report an improved methodology whereby the stabilising agent is added subsequently to the addition of gold in the synthesis as a final capping agent and can be altered to be a number of different agents including PEG, polyacrylamide (PAM), dextran, and thioglucose. This improved methodology not only provides stabilisation to the HGNs but also significantly shifts their SPR into the NIR region of the electromagnetic spectrum. This method provides much more flexibility in stabilising agents which can be used compared to the previously published method, which allows for tailoring to specific applications. A systematic investigation was then carried out to determine the most effective stabilising agent for use with HGNs which provided improved stability to a range of conditions whilst maintaining surface accessibility for small molecules so they can be used as stable red-shifted SERS substrates.

Experimental

Chemicals. Trisodium citrate dihydrate (>99%), poly(vinylpyrrolidone) (MW 10000), polyacrylamide (MW 5000000-6000000), dextran from Leuconostoc mesenteroides (MW 9000-11000), poly(ethyleneimine) (50 % (w/v) in H_2O), (3-aminopropyl)trimethoxysilane (97%), ethanol (≥99.5%), ammonium hydroxide (28.0-30.0% NH3 basis), and tetraethyl orthosilicate (99.999%) were purchased from Sigma-Aldrich. Cobalt (II) chloride hexahydrate (99.99%), sodium borohydride (99%), and chloroauric acid trihydrate (ACS reagent grade) from Acros Organics. Polyethylene glycol (CM-PEG-SH, MW 5000) was obtained from Laysan Bio Inc. and 1-Thio-β-D-glucose sodium salt dihydrate (>98%) from Santa Cruz Biotechnology.

HGN Synthesis with various stabilising agents. The synthesis developed was modified from previously reported methods.[1, 8, 22] All glassware was cleaned with aqua regia and rinsed thoroughly with deionised water before use. The synthesis was carried out under argon on a standard Schlenk line to keep the reaction free from oxygen. In a typical synthesis, trisodium citrate dihydrate (600 µL, 0.1 M) and cobalt (II) chloride hexahydrate (100 µL, 0.4 M) were added to deionised water (100 mL) in a three-necked round-bottom flask and degassed several times. While maintaining constant stirring, sodium borohydride (1 mL, 0.1 M) (freshly prepared with degassed, deionised water) was injected into the solution and left to react under argon for a further 20 minutes. At this stage the solution turned from a pale pink colour to brown indicating the formation of cobalt nanoparticles. Any remaining borohydride was quenched from the reaction mixture before the gold salt was added. Chloroauric acid trihydrate (33 mL, 0.25 mM) was then transferred into the solution, maintaining an air free environment, and stirred for a further 10 minutes. The solution was subsequently exposed to air and sodium citrate (500 µL, 0.1 M) was added as a stabilising agent. Modification of the synthesis was achieved by replacing 500 µL of 0.1 M sodium citrate with 500 µL of 1 % (w/v) CM-PEG-SH, 1 % (w/v) PVP, 1 % (w/v) PAM, 1 % (w/v) (PEI), 1 % (w/v) dextran or 1 % (w/v) 1-Thio-β-D-glucose sodium salt depending on the desired stabilising agent. Following addition of a stabilising agent the solution turned from brown to green within 5 minutes when citrate was added but increased to roughly 30 minutes when other stabilising agents were used. The resulting HGN solution was left to stir for a further two hours and was then concentrated through centrifugation (3466 g) and redispersed in 8 mL of d.H_2O for storage and further analysis.

Silica Encapsulation. To a citrate stabilized HGN solution (1 mL) was added 3-aminopropyltrimethoxysilane (APTMS) (100 µL, 20 µM). This solution was shaken for 10 minutes and left to equilibrate for a further 20 minutes. The resulting solution was centrifuged (1585 g) for 15 minutes. The silica shell was then grown using a modified Stöber's method.[23] The APTMS-HGN pellet was redispersed in a water:ethanol (1:4) solution (10 mL) and ammonia (28-30%, 160 µL) was added under stirring as a catalyst for the hydrolysis. After 5 minutes, tetraethyl orthosilicate (TEOS) (4 µL) was added in 2 equal portions over 1 hour. The mixture was left to react for 4 hours. The resultant solution was then concentrated through centrifugation (1585 g) for 15 minutes and the precipitate was redispersed in d.H_2O (1 mL) for further analysis.

Characterisation. Extinction spectroscopy was carried out on a Cary 300 Bio UV-vis spectrophotometer. Zeta potential measurements were obtained using a Malvern Zetasizer Nano ZS system. Particle sizes were obtained using ImageJ software based on the measurement of 50 particles per HGN sample. SEM samples were prepared on silicon wafers using previously reported methods.[8, 24] Briefly, wafers were washed with water and acetone, then dried under a flow of nitrogen and placed in an oxygen plasma cleaner for 60 s. Poly(diallyldimethylammonium chloride) (PDDA) solution (30 µL PDDA dissolved in 1 mL of 1 mM NaCl) was applied to the wafer and left for 30 minutes to render the surface positively charged. 50 µL of the HGN sample to be imaged was added to the wafer and left for 5-7 minutes before being removed, this process was repeated 3 times. After the third addition the sample was removed and the wafer washed with water and dried under N_2. SEM imaging was carried out on a

Hitachi S-3000N variable pressure SEM with EDX 6″ tungsten electron source at an acceleration voltage of 30 kV.

Stability Testing. HGN solutions (700 µL) were altered to acidic pH ranging from pH 2.2-2.6 with dropwise addition of citric acid (1 M) or alkaline pH ranging from pH 12.6-13.1 with dropwise addition of NaOH (1 M). Readings were recorded using a portable pH meter which was calibrated before use. HGN solutions (270 µL) were added to NaCl (300 µL, 30 mM – 1 M). Control samples were prepared using d.H2O (300 µL).

SERS Analysis. Samples for SERS analysis were prepared by mixing functionalised HGNs (135 uL) with Raman reporters: dye 1 (15 uL, 1 x 10^{-4} M) or dye 2 (15 uL, 1 x 10^{-4} M) and d.H_2O (150 uL). Samples were left for 30 minutes before SERS measurements were recorded. 1064 nm solution SERS spectra were recorded in glass cuvettes using a Real Time Analyzer FT-Raman spectrometer. Spectra were obtained by scanning 3 replicates of each sample with 20 s acquisition time under a laser incident power of 600 mW. 785 nm solution SERS spectra were recorded in a 96 well plate using a Renishaw inVia microscope system with a laser incident power of 160 mW. Each well was scanned 3 times with an accumulation time of 10 s. The signals were normalised to a cyclohexane standard. Spectra were baseline corrected using a multipoint polynomial fit and level and zero mode in Grams software (AI 7.00).

Results and Discussion

Synthesis, Characterisation and Stabilisation of HGNs.

HGNs synthesised were characterised using extinction spectroscopy, SEM imaging for confirmation of particle size and ELS for zeta potential measurements. Figure 1A shows normalised extinction spectra for HGNs synthesised using the improved methodology with various stabilising agents. It is important to note that of all the stabilising agents tried with this method, PEI was the only one found to be unsuccessful. This was thought to be due to the positively charged species causing immediate aggregation to the nanoparticles that were forming in solution. The normalised spectra clearly show that on addition of the various stabilising agents at the final stage of the HGN synthesis there is a significant red shift in the SPR of greater than 100 nm with the exception of silica where the shell was added after the initial synthesis had been completed. To highlight the reproducibility within this method citrate and silica stabilised HGNs typically had an SPR of 700 ± 50 nm, while other stabilising agents shifted the SPR to 815 ± 35 nm with the exception of thioglucose which generally had an SPR of 875 ± 25 nm. The significant red-shift and greater reproducibility agree with results previously published however this method allows extension for use with other stabilising agents which were reported to be unsuccessful when added prior to the addition of gold in the synthesis.[22] Previous studies have reported that HGNs with a SPR in the NIR region have thinner outer shells which results in a slight increase in inhomogeneity within the samples.[1, 22] This variation in shell thickness would account for the significant red-shift in SPR observed. Previous work has hypothesised that the presence of a stabilising agent could slow the growth of the gold shell and results in more red-shifted particles with thinner shells.[22] Similarly, adding the stabilising agents shortly after addition of the gold salt could hinder the development of a thicker shell whereas adding citrate aids the further reduction of the gold salt, therefore resulting in thicker shell formation. The significant increase in time taken for a colour change to occur when the various stabilising agents were added to the synthesis supports this hypothesis. HGN aggregation can be characterised by a dampening in SPR along with a shift to shorter wavelengths[25] which again suggests the red-shift observed is due to the presence of the stabilising agent and is not a result of nanoparticle aggregation.

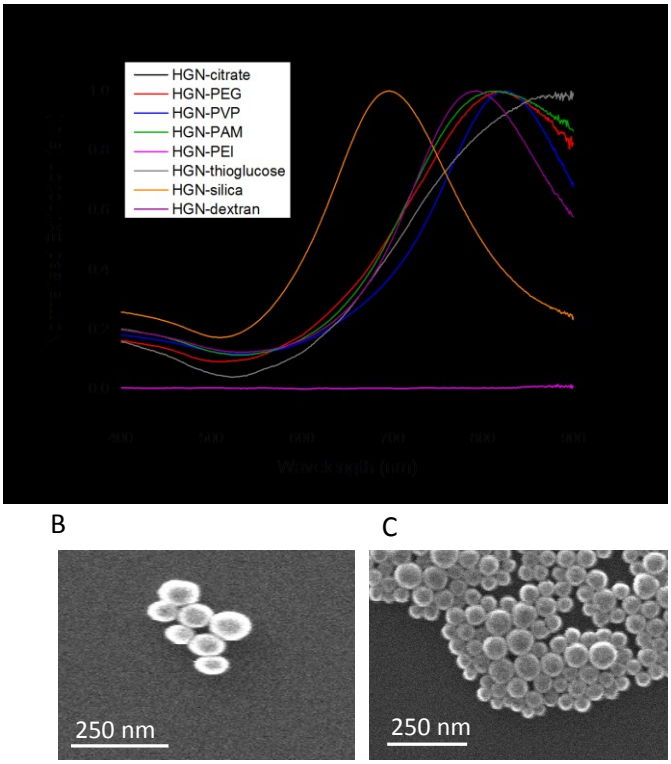

Fig. 1: (A) Normalised extinction spectra of HGNs synthesised with various stabilising agents. Spectra were normalised in order to highlight the red-shifted SPR observed in the samples with the exception of PEI which was unsuccessful and precipitated from solution. (B) SEM image of citrate-stabilised HGNs corresponding to the extinction spectrum shown in Figure 1A. (C) SEM image of PEG-stabilised HGNs corresponding to the extinction spectrum in Figure 1A.

Representative SEM images are shown in Figures 1B and 1C for citrate-stabilised and PEG-stabilised HGNs respectively. Images for the remainder of the stabilising agents used are shown in Figure S1. Particle size and ζ-potential data corresponding to the extinction spectra of the HGNs reported in Figure 1A are shown in Table 1. Particle size values observed show very little change in particle diameter within the different stabilised HGNs as the presence of the different stabilising agents cannot be observed from the SEM images. The larger standard deviation in the red-shifted HGNs indicates that there is a slight increase in inhomogeneity within these samples.

Table 1: Summary of data obtained for HGNs synthesised with various stabilising agents corresponding to extinction spectra reported in Figure 1A. Red-shift values were calculated with respect to citrate-stabilised HGNs. Zeta potential values are quoted as the mean of three replicates of each sample with error ± one standard deviation. Particle size values are calculated from the average size of 50 particles within each sample with error ± one standard deviation.

Stabilising Agent	λ_{max} (nm)	Red-Shift (nm)	Particle Size Diameter (nm)	Zeta Potential (mV)
Citrate	684	0	82.4 ± 9.6	-28.6 ± 1.2
PEG	820	136	76.5 ± 18.7	-32.9 ± 2.6
PVP	826	142	86.9 ± 18.9	-47.5 ± 2.1
PAM	811	127	87.5 ± 22.6	-21.8 ± 0.8
PEI	-	-	-	3.46 ± 0.62
Thioglucose	897	213	80.4 ± 19.3	-45.2 ± 3.1
Silica	695	11	83 ± 14.5	-38.5 ± 1.7
Dextran	791	107	84.2 ± 24	-47.7 ± 1.4

However, this is not a key issue within this study as this imparts no significant effect on the stability of the HGNs. synthesised. All stabilised-HGNs synthesised are below 100 nm, ideal for cellular uptake. PEI-stabilised HGNs showed a large increase in size when measured by DLS due to the immediate aggregation of the sample induced by the positive charge on the PEI moiety. This is supported by ζ-potential data which indicates that this is the only positive sample out of all agents tested. All other samples showed a significant degree of colloidal stability, and the difference in ζ-potential from standard citrate-HGNs indicates successful functionalisation has occurred.

HGN Stability Testing.

After incorporation of stabilising agents to the HGN synthesis the successful HGNs were systematically tested for increased tolerance to different pH and salt concentrations. Additionally, the long term stability was also investigated. We first investigated HGN tolerance to changing pH levels, which were altered by the addition of 1 M NaOH or 1 M citric acid as appropriate. Extinction spectra were recorded at the original pH of the HGN solution which ranged from pH 7.4 –9.2, acidic pH ranging from pH 2.2-2.6 and alkaline pH ranging from pH 12.6-13.1. Results for the original citrate-HGNs compared to PEG-stabilised HGNs which were found to have the most tolerance to changing conditions are shown in Figure 2. The remainder of the spectra for the additional samples tested are shown in the supplementary information Figure S2.

It is clear from Figure 2A that citrate-capped HGNs have a very limited tolerance to changing pH and precipitate from solution due to over aggregation when exposed to extreme alkaline or acidic conditions with a complete loss of plasmon band in both environments. PEG-stabilised HGNs showed a significant increased tolerance to both acidic and alkaline conditions with only a slight dampening in absorbance and very little line broadening indicating that aggregation is not taking place.

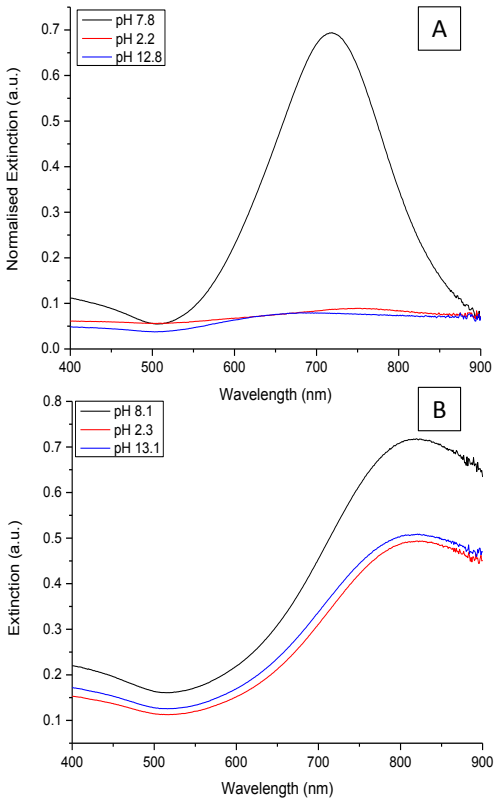

Fig. 2: Extinction spectra of (A) citrate-stabilised HGNs and (B) PEG-stabilised HGNs measured at the original pH of the nanoparticle solution (black) and acidic (red) and alkaline pH (blue). pH was altered with the addition of 1 M citric acid or 1 M NaOH and left for four hours before analysis. Spectra (A) have been normalised at 900 nm to emphasise the plasmon dampening which is occurring.

With regards to other stabilising agents used, the spectra shown in Figure S2 indicate that although there is some increased tolerance to changing conditions compared to citrate, this is not to the extent of PEG. All other materials with the exception of silica show some stability to acidic conditions however partial aggregation is indicated by the line broadening and blue-shift in SPR in the spectra. The stabilisation imparted by PEG among other agents is thought to be mainly a steric effect due to the increased stability, to not only pH, but also to increased salt concentrations. If this was a charge effect the salt would screen the charges and van der Waals attractions would induce aggregation.[26, 27]

With PEG-HGNs showing the most promising results, their tolerance to changing pH levels were studied over one month. Results observed after a 24 hour period are shown in Figure S3, these were similar to results shown in Figure 2 however the PEG tolerance to alkaline conditions has reduced. Again, citrate HGNs were sensitive to changes in conditions and precipitated from solution as before. Zeta potential measurements carried out showed that values varied significantly within different pH environments. PEG-HGNs at pH 8.1 have a ζ-potential of -41.9 ± 1.9 mV however this changes to -3.3 ± 0.5 mV at pH 2 and -24.7 ± 0.6 mV at pH 13, the inherent maintenance of stability with the significant change in ζ-potential values supports the

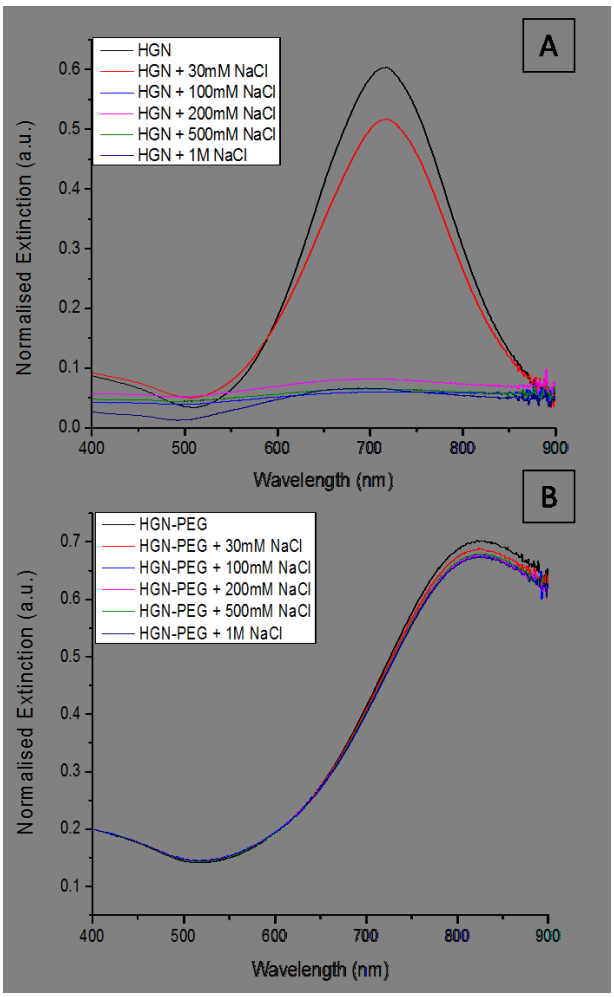

Fig. 3: Extinction spectra of (A) citrate-stabilised HGNs and (B) PEG-stabilised HGNs measured in a range of different salt concentrations (from 0 M up to 1 M NaCl). Spectra (A) have been normalised at 900 nm and (B) at 400 nm to emphasise the plasmon dampening which is occurring.

hypothesis that the stability is not solely due to charge influences but is significantly dependent on steric effects. Particle size measurements taken for PEG-HGNs were constant over the entire pH range studied showing no aggregate formation. Samples were analysed again one month after initial measurements and showed no significant change compared to results taken after 24 hours.

Salt tolerance of these nanoparticles is shown in Figure 3 for the most and least stable HGNs, with PEG-HGNs showing very little change in extinction spectra with increasing salt concentration. Results of salt tolerance in up to 1 M NaCl for the remaining HGNs synthesised can be observed in Figure S5. Here, PAM-HGNs showed only slight aggregation on addition of up to 1 M salt indicating that the stability imparted by PAM is predominantly a steric effect. PVP is slightly more tolerant than citrate in up to 100 mM salt however the decreased stability above this concentration could be due to the weaker bond formation to the HGN surface than the other polymers. Silica shelled HGNs have shown surprising results with limited stability compared to the polymers and sugars tested. Although no partial aggregation occurs when 30 mM salt was added the remaining results were similar to citrate-HGNs. This could indicate that the silica shell is too thin to provide sufficient shielding. Both sugars again showed limited stability to salt with no apparent increased stability compared to normal citrate-HGNs. Here, the steric stability may not be strong enough to overcome the screening of the charge induced by the salt. Maximum salt tolerance levels for PEG-stabilised HGNs were studied over time. Figure S4 shows salt tolerance levels in up to 5 M NaCl over 24hrs. The sustained green colour of the solution in Figure S4(b) along with the extinction spectra show that the PEG-HGNs show no sign of aggregation in up to 5 M salt. Citrate capped HGNs however, show no stability to salt as was shown previously. This is observed by both the loss of colour in solution due to nanoparticle precipitation and is supported by the extinction spectra in Figure S4(c). Measurements were repeated one month after initial analysis with very little change in results observed indicating that PEG-HGNs are stable in up to 5 M NaCl for at least one month.

Long term stability of the HGN solutions synthesised were compared, all HGN solutions were dispersed in d.H2O and stored in glass vials out of direct sunlight.

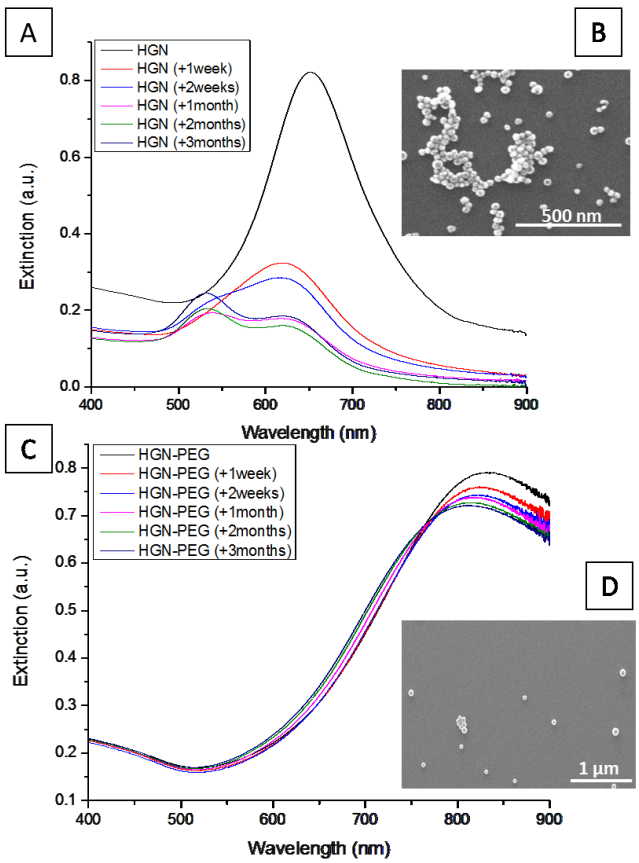

Fig. 4: Extinction spectra and corresponding SEMs of (A), (B) citrate-stabilised HGNs and (C), (D) PEG-stabilised HGNs measured at specific time intervals after initial synthesis. SEMs were taken 3 months after initial synthesis.

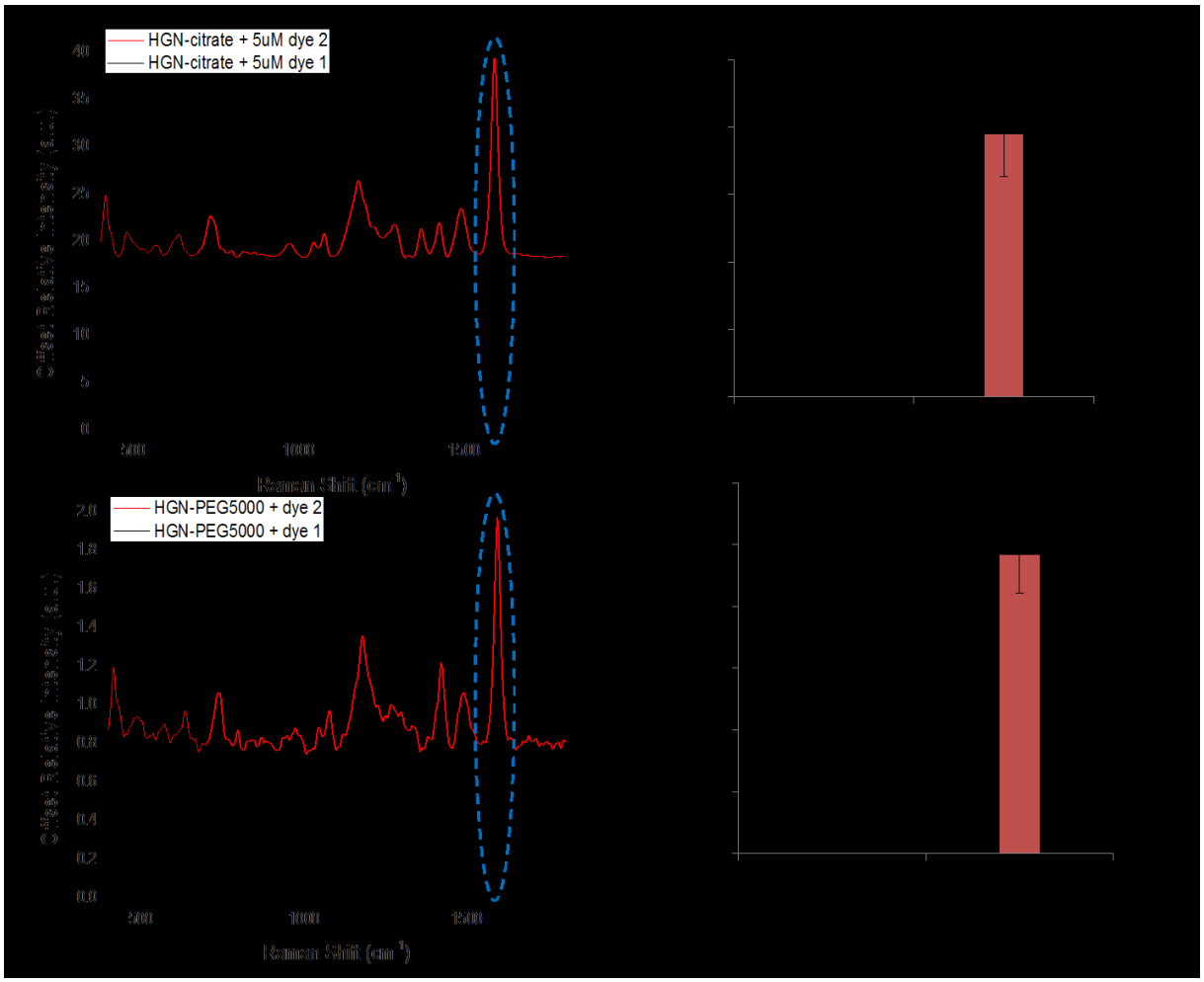

Fig. 5: SERS spectra recorded using an excitation wavelength of 1064 nm: (A) SERS spectra of dye 2 (red) and dye 1 (black) using standard citrate-HGNs; (B) SERS peak intensities at 1590 cm-1 for both reporters at 5 uM final concentration; (C) SERS spectra of dye 2 (red) and dye 1 (black) using PEG-stabilised HGNs; (D) SERS peak intensities at 1590 cm-1 for both reporters at 5 uM final concentration. Spectra were obtained by scanning 3 replicates of each sample with 20 scans averaged per sample under a laser incident power of 600 mW. Averages are shown and error bars are ± standard deviation.

Generally, citrate HGNs can be redispersed in a citrate buffer to maintain an increased stability over time however for comparison with other HGNs d.H_2O was used in this investigation. It is important to note that in citrate buffer they still do not display the same level of stability compared to PEG-HGNs redispersed in d.H_2O. Figure 4 compares the stability of citrate and PEG-stabilised HGNs over a three month period. In Figure 4A the extinction spectra for citrate-HGNs taken at specific time intervals over a three month period are shown. After just one week the SPR has significantly broadened and dampened, indicating that a significant amount of aggregation has occurred. After three months there is considerable dampening in SPR at 650 nm and a new SPR band appears at around 529 nm. This could result from an increasing number of larger aggregates and a reduction in single particles present within the sample over time. The presence of large numbers of aggregates was confirmed by SEM imaging taken after three months, an example of which is shown in Figure 4B. In contrast, PEG-HGNs are still stable after a 3-month period indicated by the lack of change in extinction spectra in Figure 4C and monodispersity in the sample shown in the SEM image in Figure 4D. Extinction spectra and corresponding SEM images for all other HGNs are shown in Figures S6 and S7. It is apparent from these that all other coatings impart a degree of stabilisation to the HGNs and maintain relatively stable solutions.

SERS Analysis.

In order to investigate the use of these stabilised HGNs as potential SERS substrates SERS analysis was carried out at two different excitation wavelengths using a newly synthesised class of Raman reporters which provide rich vibrational spectra.[28]

For analysis, reporters were added to stabilised HGNs at a final concentration of 5 uM and spectra were recorded at both 1064 nm and 785 nm laser excitation with no induced aggregation. The results using both standard citrate HGNs and PEG-stabilised HGNs at 1064 nm excitation wavelength are shown in Figure 5. The reporter labelled dye 1 is a sulphur-based compound with a λ_{max} of 789 nm and dye 2 is a structurally similar selenium-based compound with a λ_{max} of 826 nm, structures and extinction spectra are shown in Figure 6. The intensity of the prominent peak highlighted at 1590 cm^{-1} was compared. Results observed indicated that at this excitation wavelength dye 2 gave a more enhanced signal. Although the signal intensity observed using PEG-stabilised HGNs as

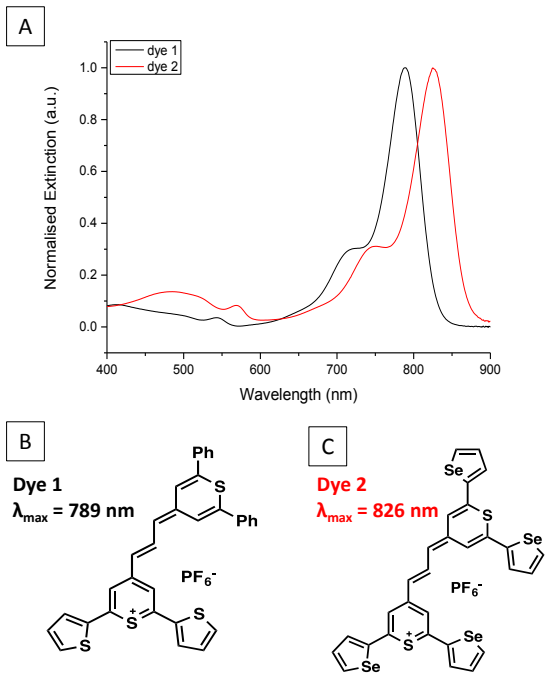

Fig. 6: (A) Normalised extinction spectra of Raman reporters dye 1 and dye 2 with a λ_{max} of 789 nm and 826 nm respectively. Structures of (B) dye 1 and (C) dye 2.

substrates was significantly weaker than the citrate HGN substrates it was still readily distinguishable and showed a vast improvement on other commercially available Raman reporters such as 1,2-bis(2-pyridyl)ethylene (BPE) where no signal was apparent (data not shown). The reduction in signal was due to the presence of the stabilising agent which hinders adsorption of reporters on the HGN surface and therefore reduces the enhancement effect provided from the metal surface. In addition to this we stated previously that the red-shifted stabilised HGNs possess a thinner gold shell than standard citrate HGNs. Thinner shells have a lower outer electric field compared to thicker shells[29] so therefore the reduction in signal could also be due to the weaker electric field distribution in the stabilised HGNs. SERS spectra were recorded for all stabilising agents used and are shown in Figure S8. The general trend observed across all stabilising agents investigated showed dye 2 gave the greatest enhancement at 1064 nm excitation wavelength. Figure S8C shows PEG-stabilised HGNs provided the least enhanced signals out of all stabilising agents used, however other coatings were previously shown to be less stable and addition of reporter molecules induced aggregation in the samples which enhanced the SERS signals. This limits future applications where stable substrates are required.

We then repeated this experiment at a laser excitation of 785 nm. Dye 1 is resonant at 789 nm and therefore an extra enhancement from the dye was expected at this wavelength. Results observed are shown in Figure S9 and by comparing the prominent peak at 1600 cm^{-1} as before it is clear that dye 1 shows a greater enhancement at this wavelength as expected. This general trend can again be observed across all stabilised HGNs and is shown in Figure S10.

Conclusions

In this work we have presented an improved method for HGN synthesis which both improves the stability and shifts the SPR to longer wavelengths making them advantageous for use in many biomedical applications where nanostructures with a SPR in the NIR region are desirable. In addition to this we have systematically compared the stability of three different materials commonly used as stabilising agents and tested their tolerance to different salt and pH environments. The results indicated that in regards to HGNs, PEG is the most suitable stabilising agent increasing stability to high salt concentrations and pH extremes with an inherent stability over one month in up to 5 M NaCl and in both acidic and alkaline environments. Additionally, HGNs stabilised with PEG provide greater long term stability to the nanoparticles with no reduction in stability over at least three months. We have also achieved SERS of stabilised HGNs at both 785 nm and 1064 nm excitation using a newly synthesised class of Raman reporter molecules. Overall, PEG-stabilised HGNs synthesised within this work possess a combination of increased stability across a range of environments, long term stability and SERS signals in the NIR region making them excellent SERS substrates for potential use in many biomedical applications.

Acknowledgements

This work was supported by Dstl and the Engineering and Physical Sciences Research Council [grant number EP/J500550/1]. The research data associated with this paper will become available at the following link from Jan 2015 https://pure.strath.ac.uk/portal/en/projects/epsrc-doctoral-training-grant(288fce07-0618-470d-8f27-af9f3db358ea).html
DG acknowledges the Royal Society for support in the form of a Wolfson Research Merit Award.

Notes and references

[a] *Centre for Molecular Nanometrology, WestCHEM, Department of Pure and Applied Chemistry, University of Strathclyde, 295 Cathedral Street, Glasgow, G1 1XL, United Kingdom.*
E-mail: Duncan.graham@strath.ac.uk
[b] *Dstl Porton Down, Salisbury, Wiltshire, SP4 0JQ, UK.*
[c] *Department of Chemistry, University at Buffalo, The State University of New York, New York 14260, United States.*

† Electronic Supplementary Information (ESI) available: [details of any supplementary information available should be included here]. See DOI: 10.1039/b000000x/

1. A. M. Schwartzberg, T. Y. Olson, C. E. Talley and J. Z. Zhang, *J. Phys. Chem. B*, 2006, **110**, 19935-19944.
2. E. Hutter and J. H. Fendler, *Adv. Mater.*, 2004, **16**, 1685-1706.
3. W. Lu, C. Xiong, G. Zhang, Q. Huang, R. Zhang, J. Z. Zhang and C. Li, *Cancer Res.*, 2009, **15**, 876-886.
4. J. Z. Zhang and C. Noguez, *Plasmonics*, 2008, **3**, 127-150.
5. H. P. Liang, L. J. Wan, C. L. Bai and L. Jiang, *J. Phys. Chem. B*, 2005, **109**, 7795-7800.
6. H. Xie, I. A. Larmour, Y.-C. Chen, A. W. Wark, V. Tileli, D. W. McComb, K. Faulds and D. Graham, *Nanoscale*, 2013, **5**, 765-771.
7. J. You, G. Zhang and C. Li, *ACS nano*, 2010, **4**, 1033-1041.

8. H. Xie, I. A. Larmour, W. E. Smith, K. Faulds and D. Graham, *J. Phys. Chem. C*, 2012, **116**, 8338-8342.
9. R. Weissleder, *Nat. Biotechnol.*, 2001, **19**, 316-316.
10. V. Vongsavat, B. M. Vittur, W. W. Bryan, J. H. Kim and T. R. Lee, *ACS Appl. Mater. Interfaces*, 2011.
11. D. Schmaljohann, *Adv. Drug Deliv. Rev.*, 2006, **58**, 1655-1670.
12. B. D. Chithrani, A. A. Ghazani and W. C. Chan, *Nano Lett.*, 2006, **6**, 662-668.
13. X. Wang, G. Li, T. Chen, M. Yang, Z. Zhang, T. Wu and H. Chen, *Nano Lett.*, 2008, **8**, 2643-2647.
14. L. C. Martin, I. A. Larmour, K. Faulds and D. Graham, *Chem. Commun.*, 2010, **46**, 5247-5249.
15. S. Watanabe, H. Seguchi, K. Yoshida, K. Kifune, T. Tadaki and H. Shiozaki, *Tetrahedron Lett.*, 2005, **46**, 8827-8829.
16. F. Geng, K. Song, J. Z. Xing, C. Yuan, S. Yan, Q. Yang, J. Chen and B. Kong, *Nanotechnology*, 2011, **22**, 285101.
17. S. Liu and M. Han, *Adv. Funct. Mater.*, 2005, **15**, 961-967.
18. J. Huang, K. H. Kim, N. Choi, H. Chon, S. Lee and J. Choo, *Langmuir*, 2011, **27**, 10228-10233.
19. S. P. Mulvaney, M. D. Musick, C. D. Keating and M. J. Natan, *Langmuir*, 2003, **19**, 4784-4790.
20. W. E. Doering and S. Nie, *Anal. Chem.*, 2003, **75**, 6171-6176.
21. B. Küstner, M. Gellner, M. Schütz, F. Schöppler, A. Marx, P. Ströbel, P. Adam, C. Schmuck and S. Schlücker, *Angew. Chem. Int. Ed.*, 2009, **48**, 1950-1953.
22. S. Preciado-Flores, D. Wang, D. A. Wheeler, R. Newhouse, J. K. Hensel, A. Schwartzberg, L. Wang, J. Zhu, M. Barboza-Flores and J. Z. Zhang, *J. Mater. Chem.*, 2011, **21**, 2344-2350.
23. W. Stöber, A. Fink and E. Bohn, *J. Colloid Interface Sci.*, 1968, **26**, 62-69.
24. H. Xie, I. A. Larmour, V. Tileli, A. L. Koh, D. W. McComb, K. Faulds and D. Graham, *J. Phys. Chem. C*, 2011, **115**, 20515-20522.
25. K. L. Knappenberger, Jr., A. M. Schwartzberg, A. M. Dowgiallo and C. A. Lowman, *J. Am. Chem. Soc.*, 2009, **131**, 13892-13893.
26. I. A. Larmour, K. Faulds and D. Graham, *J. Phys. Chem. C*, 2010, **114**, 13249-13254.
27. N. J. Lang, B. Liu, X. Zhang and J. Liu, *Langmuir*, 2013, **29**, 6018-6024.
28. M. A. Bedics, H. Kearns, J. M. Cox, S. Mabbott, F. Ali, N. C. Shand, K. Faulds, J. B. Benedict, D. Graham and M. R. Detty, *Chem. Sci.*, 2015, DOI: 10.1039/C4SC03917C.
29. M. Chandra, A.-M. Dowgiallo and K. L. Knappenberger Jr, *J. Am. Chem. Soc.*, 2010, **132**, 15782-15789.

